Mechanistic Studies of Improved Foam EOR Processes

Semi-Annual Report for the Period
September 1, 2001 – February 28, 2002

Principal Author:

William R. Rossen

Date Report Issued: January 28, 2003

Work Performed under Contract DE-FC26-01BC15318

The University of Texas at Austin
Center for Petroleum and Geosystems Engineering
1 University Station, C0300
Austin, TX 78712-1061

DISCLAIMER

Mechanistic Studies of Improved Foam EOR Processes

Contract No. DE-FC26-01BC15318

The University of Texas at Austin
1 University Station, C0300
Austin, TX 78712-1061

Contract Date: Sept. 1, 2001
Anticipated Completion: Aug. 31, 2004

ABSTRACT:

The objective of this research is to widen the application of foam to enhanced oil recovery (EOR) by investigating fundamental mechanisms of foams in porous media. This research will lay the groundwork for more applied research on foams for improved sweep efficiency in miscible gas, steam and surfactant-based EOR. Task 1 investigates the pore-scale interactions between foam bubbles and polymer molecules. Task 2 examines the mechanisms of gas trapping, and interaction between gas trapping and foam effectiveness. Task 3 investigates mechanisms of foam generation in porous media.

The most significant progress during this period was made on Tasks 2 and 3.

Research on Task 2 focused on simulating the effect of gas trapping on foam mobility during foam injection and during subsequent injection of liquid. Gas trapping during liquid injection is crucial both to injectivity during liquid injection in surfactant-alternating-gas foam (SAG) projects and also provides a window into trapping mechanisms that apply during foam flow.

We updated our simulator for foam (Rossen *et al*., 1999; Cheng *et al*., 2000) to account explicitly for the first time for the effects of gas trapping on gas mobility in foam and in liquid injected after foam, and for the effects of pressure gradient on gas trapping. The foam model fits steady-state foam behavior in both high- and low-quality flow regimes (Alvarez *et al*., 2001) and steady-state liquid mobility after foam. The simulator also fits the transition period between foam and liquid injection in laboratory corefloods qualitatively with no additional adjustable parameters.

Research on Task 3 focused on foam generation in homogeneous porous media. In steady gas-liquid flow in homogeneous porous media with surfactant present, there is often observed a critical injection velocity or pressure gradient ∇p^{min} at which foam generation occurs. Earlier research on foam generation was extended with extensive data for a variety of porous media, permeabilities, gases (N_2 and CO_2), surfactants, and temperatures. For bead- and sandpacks, ∇p^{min} scales like (1/k), where k is permeability, over 2½ orders of magnitude in k; for consolidated media, the relation is more complex. For dense-CO_2 foam, ∇p^{min} exists but can be less than 1 psi/ft. If pressure drop, rather than flow rates, is fixed, one observes an unstable regime between stable "strong" and "coarse" foam regimes; in the unstable regime ∇p is nonuniform in space or variable in time. Results are interpreted in terms of the theory of foam mobilization at a critical pressure gradient (Rossen and Gauglitz, 1990).

TABLE OF CONTENTS

OBJECTIVES

The objective of this research is to widen the application of foam to enhanced oil recovery (EOR) by investigating fundamental mechanisms of foams in porous media. This research will lay the groundwork for more applied research on foams for improved sweep efficiency in miscible gas, steam and surfactant-based EOR. Task 1 investigates the pore-scale interactions between foam bubbles and polymer molecules. Task 2 examines the mechanisms of gas trapping, and interaction between gas trapping and foam effectiveness. Task 3 investigates mechanisms of foam generation in porous media.

RESULTS AND DISCUSSION

TASK 1: INTERACTIONS BETWEEN POLYMER AND FOAM

A graduate research assistant was recruited and began working on this area. No significant results were obtained on this task during this period.

TASK 2: GAS TRAPPING

Research on Task 2 focused on simulating the effect of gas trapping on foam mobility during foam injection and during subsequent injection of liquid. Gas trapping during liquid injection is crucial both to injectivity during liquid injection in surfactant-alternating-gas foam (SAG) projects and to acid diversion in well stimulation. In the recent foam field trial at the Snorre field, low injectivity during liquid-slug injection caused fracturing and the loss of all subsequently injected surfactant (Blaker, *et al*., 1999). This low injectivity is a result of gas trapping by the liquid slug. Injectivity of liquid after foam is also a window into trapping mechanisms that apply during foam flow.

We updated our foam simulator (Rossen *et al*., 1999; Cheng *et al*., 2000) to account explicitly for the first time for the effects of gas trapping on gas mobility in foam and in liquid injected after foam, and for the effects of pressure gradient on gas trapping (Cheng *et al*., 2002). The procedure is as follows: Rossen and Wang (1999) provide data for liquid mobility at steady-state during post-foam liquid injection, when all gas remaining is trapped. Assuming a plausible liquid relative-permeability function, this implies the trapped-gas saturation with foam S_{gr}^f as a function of pressure gradient ∇p, shown in Fig. 1. The crucial assumption of this work is that this function applies to gas trapping in steady-state foam flow as well. The relative-permeability function for gas then incorporates this function $S_{gr}^f(\nabla p)$ rather than a fixed, constant value of S_{gr} as in the previous model. The other parameters in the model must be recalculated given the new functional form for S_{gr}^f. A detailed procedure for fitting the parameters is given in Cheng *et al*. (2002) and Cheng's dissertation (2002).

The foam model fits steady-state foam behavior in both high- and low-quality flow regimes (Alvarez *et al*., 2001) and steady-state liquid mobility after foam. Previously, laboratory experiments suggested a relatively slow transition between steady states during foam and liquid injection. The simulator fits this transition period in laboratory corefloods qualitatively with no additional adjustable parameters.

The dynamics in the transition period are complex. For instance, simulations indicate that most of the core experiences a period of drier flow at the start of liquid injection, due to expansion of gas already in the core. Simulations and data agree that the transition is faster at higher pressure (with lower gas compressibility) and that response to a shut-in period depends on how much gas escapes during the shut-in - i.e., on how long the shut-in lasts.

Extended to radial flow, the simulator suggests that the transition period may not be so crucial in field application as at first appeared from laboratory corefloods. In the cases examined, injection-well pressure approaches its steady-state value within about 15 minutes or less of the start of liquid after foam.

We also found experimental artifacts that have altered previous studies of liquid injectivity after foam. Specifically, a foam generator and associated tubing and fittings upstream of the core in most previous coreflood studies acts as a "dead volume" during liquid injection that can significantly affect the results and especially the transition period. Simulations suggest that this dead volume is the cause of the simultaneous decline in pressure gradient in all sections of the core observed in previous studies. New laboratory experiments without the dead volume qualitatively confirm several of the trends predicted by simulation.

TASK 3: FOAM GENERATION

In steady gas-liquid flow in homogeneous porous media with surfactant present, there is often observed a critical injection velocity or pressure gradient ∇p^{min} at which "weak" or "coarse" foam is abruptly converted into "strong foam," with a reduction of one to two orders of magnitude in total mobility: i.e., "foam generation" (Ransohoff and Radke, 1988; Rossen and Gauglitz, 1990; Tanzil *et al*., 2001; Friedmann *et al*., 1991; Friedmann *et al*., 1994; Shi, 1996). Once foam generation is obtained, one can reduce injection rates and maintain strong foam. See Fig. 2. Earlier research on foam generation was extended with extensive data for a variety of porous media, permeabilities, gases (N_2 and CO_2), surfactants, and temperatures. Unlike most previous studies, these experiments were conducted with fixed pressure drop across the core or sandpack, rather than fixed injection rates. As a result, one observes not only the "coarse foam" with low pressure gradient and "strong foam" with high pressure gradient, but an unstable transient regime between them, as illustrated in Fig. 3.

Similar experiments were conducted with N_2 and CO_2, many surfactant formulations and porous media ranging from consolidated cores to high-permeability beadpacks. The results correlating ∇p^{min} with permeability of the medium are summarized in Fig. 4. As shown in Fig. 4, in beadpacks and sandpacks, ∇p^{min} was seen to vary with permeability k as (1/k) over 2½ orders of magnitude in k. The relation between ∇p^{min} and k is more complex in consolidated media, in part because the relations between permeability, pore-throat size and pore length are more complex. This scaling of ∇p^{min} with (1/k) implies that foam generation scales with pore-throat radius and with the length of some sort of pore cluster, not the length of the medium.

Finite values of ∇p^{min} were observed for CO_2 foams (Fig. 4). ∇p^{min} was under 1 psi/ft, however, easily attainable in the field. ∇p^{min} was a factor of 20 lower with CO_2 than with N_2 foams under similar conditions. Part, but not all, of this difference can be explained by the lower surface tension with dense CO_2.

The unstable regime at values of ∇p intermediate between coarse and strong foam (Fig. 3) is particularly interesting. This regime manifests its instability in fluctuating flow rates at fixed ∇p, and, at least sometimes, in ∇p that is not uniform. Some field applications of foam place limits on injection-well pressure, and therefore limit ∇p in the foam bank. These field applications may be constrained to operate in this unstable regime. It important to determine how this instability, that appears as fluctuations in time in a 1D experiment, would appear in 3D - for instance, possibly as fluctuating regions in space within a foam bank.

For a given surfactant formulation and porous medium, it appears that there is one continuous surface of ∇p as a function of flow rates of liquid and gas, shown schematically in Fig. 5. There is low ∇p with coarse foam. At the onset of foam generation this surface folds over (*cf*. Fig. 3) to form an intermediate "transient" regime that is unstable, folding back to form the steady-state strong-foam regime at higher ∇p. It is this upper surface that one observes in studies of the low-quality and high-quality steady-state strong-foam regimes (Alvarez *et al*., 2001). The appearance of this folding surface is similar to that observed in "catastrophe theory" for dynamic systems with multiple steady states (Poston and Stewart, 1978).

Detailed results are presented in SPE 75177, prepared for presentation at the SPE Annual Technical Conference and Exhibition in San Antonio, TX, in Oct. 2002 (Gauglitz *et al*., 2002a); this paper later appeared substantially the same form in the journal *Chem. Eng. Sci*. (Gauglitz *et al*., 2002b).

REFERENCES

Alvarez, J. M., Rivas, H., and Rossen, W. R.: "A Unified Model for Steady-State Foam Behavior at High and Low Foam Qualities," *SPE J* (Sept. 2001), 325-333.

Blaker, T., Celius, H.K., Lie, T., Martinsen, H.A., Rasmussen, L. and Vassenden, F.: “Foam for Gas Mobility Control in the Snorre Field: The FAWAG Project,” paper SPE 56478 presented at the 1999 SPE Annual Technical Conference and Exhibition, Houston, TX, Oct. 3-6.

Cheng, L.: “Simulation Studies of Foam-Acid Diversion,” PhD dissertation, Department of Petroleum and Geosystems Engineering, The University of Texas at Austin, 2002.

Cheng, L., Kam, S. I., Delshad, M., and Rossen, W. R.: "Simulation of Dynamic Foam-Acid Diversion Processes," *SPE J* (Sept. 2002), 316-324.

Cheng, L., Reme, A. B., Shan, D., Coombe, D. A., and Rossen, W. R., "Simulating Foam Processes at High and Low Foam Qualities," paper SPE 59287 presented at the 2000 SPE/DOE Symposium on Improved Oil Recovery, Tulsa, OK, 3-5 April.

Friedmann, F., Chen, W. H., and Gauglitz, P.A.: "Experimental and Simulation Study of High-Temperature Foam Displacement in Porous Media," SPERE (Feb. 1991) 37-45.

Friedmann, F., Smith, M. E., Guice, W. R., Gump, J. M., and Nelson, D. G.: "Steam-Foam Mechanistic Field Trial in the Midway-Sunset Field," SPERE (Nov. 1994), 297-304.

Gauglitz, P. A., Friedmann, F., Kam, S. I., and Rossen, W. R.: "Foam Generation in Porous Media," paper SPE 75177 presented at the 2002a SPE/DOE Symposium on Improved Oil Recovery, Tulsa, OK, 13-17 April.

Gauglitz, P.A., Friedmann, F., Kam, S.I, and Rossen, W.R., “Foam Generation in Homogeneous Porous Media,” Chem. Eng. Sci. 57, 4037-4052 (2002b).

Poston, T. and Stewart, I.: Catastrophe Theory and Its Applications, Dover Publications, Inc., Mineola, (1978).

Ransohoff, T. C., and Radke, C. J.: "Mechanisms of Foam Generation in Glass-Bead Packs," SPERE (May 1988), 573-585.

Rossen, W. R., and Gauglitz, P. A.: "Percolation Theory of Creation and Mobilization of Foam in Porous Media," AIChE J. 36 (1990), 1176-1188.

Rossen, W.R., Zeilinger, S.C., Shi, J.-X., and Lim, M. T.: "Simplified Mechanistic Simulation of Foam Processes in Porous Media," SPE J, 4, 279-287 (Sept. 1999).

Shi, J.-X: "Simulation and Experimental Studies of Foam for Enhanced Oil Recovery," PhD dissertation, Department of Petroleum and Geosystems Engineering, The University of Texas at Austin, 1996.

Tanzil, D: "Foam Generation and Propagation in Heterogeneous Porous Media," Ph.D. dissertation, Department of Chemical Engineering, Rice U., 2001.

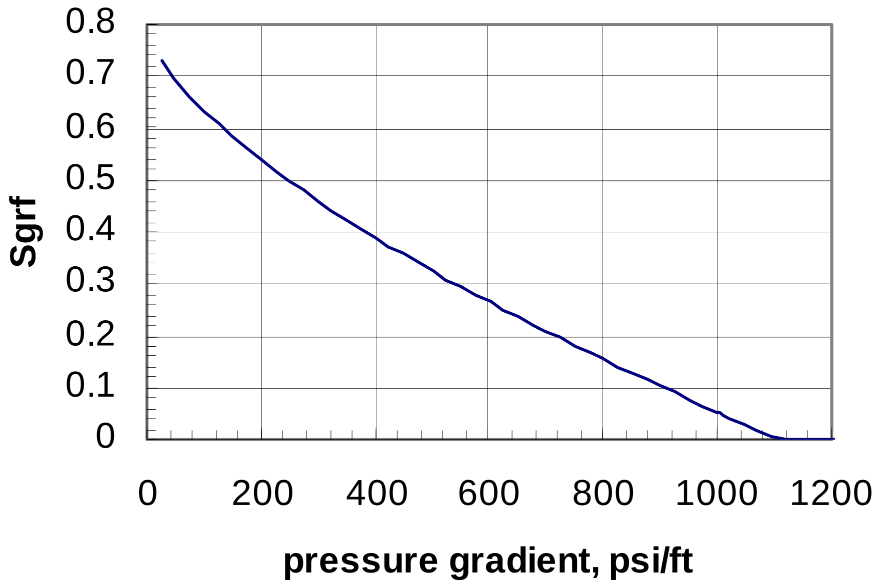

Fig. 1. Trapped-gas saturation with foam S_{gr}^{f} as a function of pressure gradient ∇p, fit to data of liquid mobility during post-foam injection.

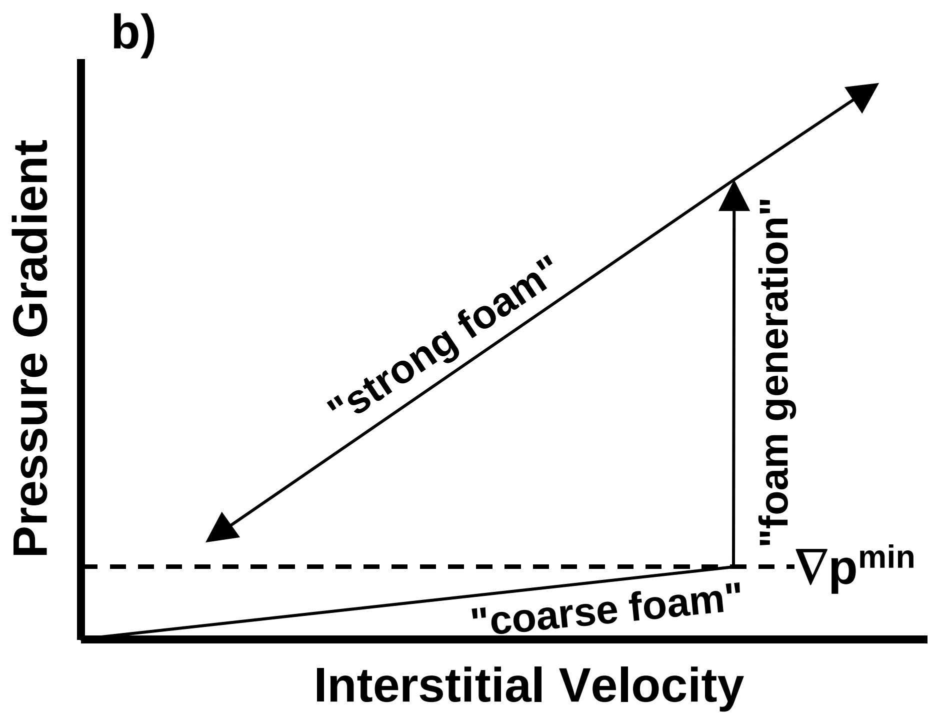

Fig. 2. Schematic of minimum pressure gradient for foam generation as seen in experiments at a fixed injection rate that is steadily increased; relation between pressure gradient and interstitial velocity.

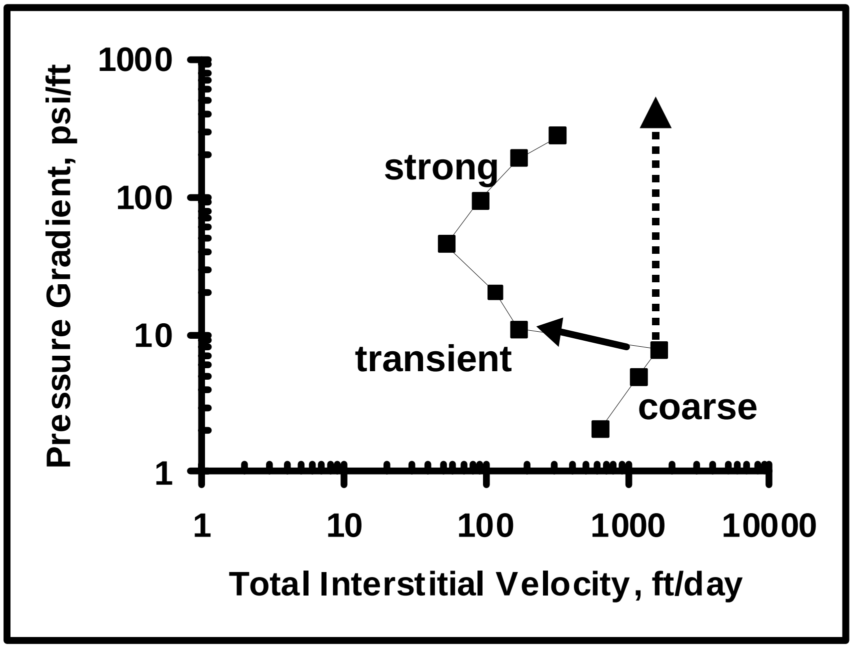

Fig. 3. Total interstitial velocity as a function of pressure gradient for one surfactant formulation in Boise sandstone. Dark arrow indicates start of foam generation in experiment with fixed pressure drop across core. Dotted arrow indicates sudden rise in pressure gradient that would be observed upon foam generation in an experiment at fixed injection rates.

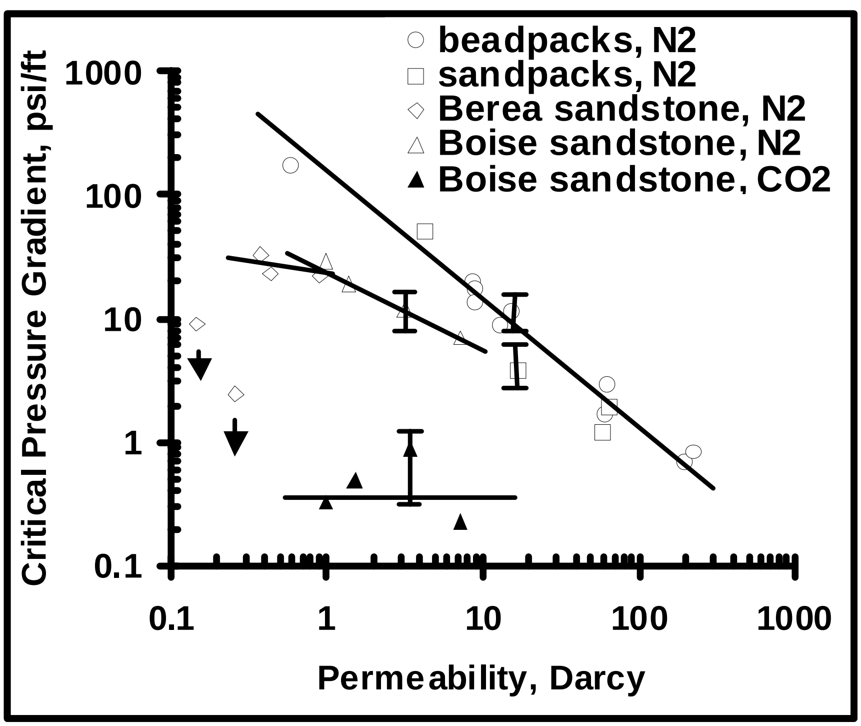

Fig. 4. Minimum pressure gradient for foam generation as a function of permeability for several N_2 and CO_2 foams.

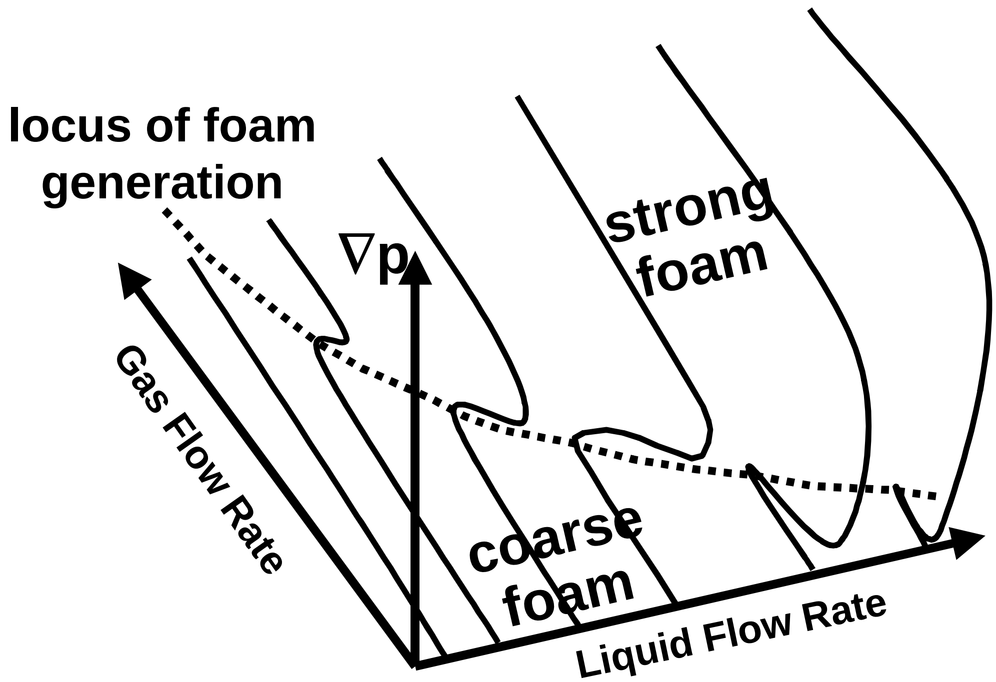

Fig. 5. Schematic of surface defining pressure gradient as function of injection rates of liquid and gas, locus of foam generation at folding of this surface, and coarse-foam and strong-foam regimes. Solid curves schematically represent data at fixed liquid flow rate.